Electronic Supplementary Material (ESI) for New Journal of Chemistry.

Supporting Information for

Aggregation Induced Emission Enhancement (AIEE) of Tripodal Pyrazole Derivatives for Sensing for Nitroaromatics; Vapor Phase Detection of Picric Acid.

Shambhu Kandel,[a] Veerasamy Sathish,[a,b] Logesh Mathivathanan,[a] Alexander N. Morozov,[a] Alexander M. Mebel,[a] Raphael G. Raptis[a,*]

[a] Department of Chemistry and Biochemistry and Biomolecular Sciences Institute, Florida International
University, 11200 SW 8th St, Miami, FL 33199, USA

[b] Department of Chemistry, Bannari Amman Institute of Technology, Sathyamangalam 638 401, India

Contents

Experimental Section

All chemicals were purchased from Sigma-Aldrich, Alfa Aesar or Fisher Scientific Co., and used as received. Reagent grade solvents were used without further purification. 1,3,5-tris(bromomethyl)-2,4,6-triethylbenzene[1] and 4-phenyl-1*H*-pyrazole[2] were synthesized by literature procedures. 4- (3- chlorophenyl)-1*H*- Pyrazole and 4- (4- nitrophenyl)-1*H*- Pyrazole were synthesized similarly to 4-phenyl-1*H*-pyrazole[2] but, using the 3-chloro-phenylacetic acid and 4-nitro-phenylacetic acid, respectively. ^{1}H-NMR spectra were recorded on a 400 MHz Bruker Avance spectrometer. FT-IR spectra were recorded with an Agilent Cary 600 FTIR. Elemental analyses were carried out by Galbraith Laboratories, Inc., Knoxville, TN, USA.

Electronic absorption spectra were recorded on an Agilent Cary 5000 UV-vis-NIR spectrophotometer using 1 cm path length cuvette. Emission spectral studies of solutions and fluorescent test strips were carried out using an Agilent fluorometer using an excitation and emission bandwidth of 2.5 nm. The fluorescent test strips were prepared by dip coating of trispyrazole compounds, followed by air drying. The morphology of the nano-aggregates was studied by dynamic light scattering spectroscopy using Carl Zeiss. SEM images were recorded with a TESCAN VEGA3 instrument using a SE detector and equipped with an EDAX energy-dispersive X-ray spectroscopy (EDX) detector. HPLC grade THF and double distilled water were employed in all spectral measurements. Freshly prepared sample solutions were used for each measurement. The detection limit can be calculated by previous literature.[3]

Frequency-domain fluorescence lifetime measurements were performed using a ChronosFD spectrofluorometer (ISS, Champaign, IL). Samples were excited with a 280 nm modulated diode, and emission was collected using 305 nm long-pass filters (Andover, Salem, NH). All measurements were conducted at room temperature in quartz cells. Modulation-phase data were analyzed using GlobalsWE software, and the $\chi 2$ parameter was used as goodness-of-fit criterion. The average intensity decay lifetime was obtained by fitting the data to a multiple-exponential decay model.

X-ray diffraction data were collected with Bruker D8 Quest diffractometer. Colorless single crystals of **1-5** and ligand-PA compounds were obtained by recrystallization from organic solvents such as acetone and/or dichloromethane. A suitable crystal for each compound was selected and mounted on a Mitegen loop using Parabar oil on a Bruker D8 Quest CMOS diffractometer. The crystal was kept at room temperature during data collection. Using **APEX3,** the structure was solved with the **ShelXT**[4] structure solution program, using the intrinsic phasing method. Using Olex2[5], the model was refined with version 2016/6 of **ShelXL**[6] using full matrix least squares on $\mathbf{F^2}$ minimization. A multi-scan absorption correction was performed using SADABS-2016/2 (Bruker, 2016/2) was used for absorption correction. All non-hydrogen atoms were refined anisotropically. Hydrogen atom positions were calculated geometrically and refined using the riding model, but some hydrogen atoms were refined freely. Disordered solvent electron densities were removed using SQUEEZE routine (PLATON)[7] or Solvent MASK (Olex2)[5] from compounds [**5**] and [**3**]-$PA_{(1:2)}$.

Computational Details:

Geometry optimization of the complexes of trispyrazole with one, two and three molecules of picric acid have been performed using a density functional ωB97XD method developed by Head-Gordon's group,[8] which includes a correction for dispersion, with the 6-31G* basis set. Next, single point time dependent density functional theory (TD-DFT)[9] calculations were carried out at the optimized geometries to evaluate electronic excitation energies and oscillator strengths. All electronic structure calculations were carried out using the GAUSSIAN 09 program package.[10]

Synthesis and Characterization of trispyrazoles

Synthesis of tris(4-Ph-pz); ($C_{42}H_{42}N_6$) [1]

A round bottom flask was charged with NaOH (250 mg), 4-(phenyl)-1H-pyrazole (385 mg; 1.75 mmol) and 15 mL of dimethylforamide (DMF) and the reaction mixture was stirred for 40 min. 1,3,5-tris(bromoethyl)-2,4,6-triethyl benzene (220 mg; 0.5 mmol) was added, the reaction mixture was heated for 36 h at 70 °C and the hot contents of the flask were poured into 50 mL cold water; the white, spongy solid that formed was refrigerated overnight. The white product was filtered out under suction and washed with water, followed by diethylether. Finally, the compound was re-dissolved in the minimal volume of dichloromethane, crushed out by hexane and dried. Yield: 284 mg (90 %). Molecular weight: 630.84 g/mol. ^{1}H-NMR (ppm, DMSO-d^6): 0.88 (9H, t, $^3J_{HH}$ = 7.4 Hz, CH_3); 2.88 (6H, q, $^3J_{HH}$ = 7.2 Hz, CH_2); 5.44 (6H, s, CH_2); 7.16 (3H, t, $^3J_{HH}$ = 7.3 Hz, phenyl); 7.29 (6H, t, $^3J_{HH}$ = 7.6 Hz, phenyl); 7.51 (6H, d, $^3J_{HH}$ = 7.8 Hz, phenyl); 7.89 (3H, s, pz); 7.96 (3H, s, pz). IR (υ_{max} cm^{-1}): 3060(w), 2976(w), 1658(w), 1608(w), 1564(m), 1491(w), 1456(w), 1554(w), 1367(m), 1336(m), 1298(w), 1228(w), 1176(s), 1068(w), 994(s), 952(s), 752(s), 688(s), 583(w). Elemental analysis; found (%) C = 79.79, H = 6.35, N = 13.31; calculated (%) C = 79.97, H = 6.71, N = 13.32. X-ray quality single crystals were grown by slow evaporation from acetone or dichloromethane solutions.

Synthesis of Tris-4-(3-Cl-Ph-pz); ($C_{42}H_{39}N_6Cl_3$) [3]
Similarly to the synthesis of **1**, but, using 4-(3-Cl-Ph)pzH (312 mg; 1.75 mmol) as a pyrazole; Yield: 327 mg (89%). Molecular weight: 734.17 g/mol. ^{1}H-NMR (ppm, $CDCl_3$): 1.02 (9H, t, $^3J_{HH}$ = 7.5 Hz, CH_3); 2.83 (6H, q, $^3J_{HH}$ = 7.5 Hz, CH_2); 5.50 (6H, s, CH_2); 7.15 – 7.25 (9H, m, phenyl), 7.37 (3H, s, phenyl) ; 7.33 (3H, s, pz) 7.81 (1H, s, pz). IR (υ_{max} cm^{-1}): 3109(w), 2979(w), 1679(w), 1604(s), 1568(m), 1465(m), 1351(m), 1179(s), 1078(m), 1067(s), 993(m), 858(s), 771(s), 666(s), 588(m). Elemental analysis for the Tris [4-(3-Cl-Ph)-pz] was found (%) C = 67.55, H = 5.52, N = 11.12; Calculated (%) C = 67.07, H = 5.49, N = 11.17. X-ray quality sinlge crystals were grown by slow evaporation from an acetone solution.

Synthesis of Tris-4-(4-NO$_2$-phenyl-pz); ($C_{42}H_{39}N_9O_6$) [4]
Similarly to the synthesis of **1**, but, 4-(4-NO$_2$-Ph)pz (332 mg; 1.75 mmol) as a pyrazole; Yield: 325 mg (85%). Molecular weight: 765.83g/mol. ^{1}H-NMR (ppm, $CDCl_3$): 1.05 (9H, t, $^3J_{HH}$ = 7.5 Hz, CH_3); 2.85 (6H, q, $^3J_{HH}$ = 7.5 Hz, CH_2); 5.53 (6H, s, CH_2); 7.51 (6H, d, $^3J_{HH}$ = 8.8 Hz, phenyl); 8.12 (6H, d, $^3J_{HH}$ = 8.8 Hz, phenyl); 7.53 (3H, s, pz); 7.89 (3H, d, pz). IR (υ_{max} cm^{-1}): 3115(w), 2977(m), 1672(w), 1598(s), 1589(m), 1500(s), 1442(w), 1330(s), 1227(m), 1194(m), 1110(s), 1069(m), 994(m), 952(s), 846(s), 753(s), 693(m), 590(m). Elemental analysis for the TPZ [4-(4-NO$_2$-Ph)-pz] ($C_{42}H_{39}N_9O_6$) was found (%) C = 62.50, H = 5.08, N = 15.51; Calculated (%) C = 62.91, H = 5.41, N = 15.72. X-ray quality single crystals were grown by slow evaporation from acetone or dichloromethane solution.

Synthesis of tris(4-I-pz) ($C_{24}H_{27}N_6I$) [5]
Similarly to the synthesis of **1**, but, using 4-(iodo)-1H-pyrazole (339 mg; 1.75 mmol) as a pyrazole; Yield: 351 mg (90%). Molecular weight: 780.24g/mol. ^{1}H-NMR (ppm, $CDCl_3$): 0.93 (9H, t, $^3J_{HH}$ = 7.6 Hz, CH_3); 2.70 (6H, q, $^3J_{HH}$ = 7.6 Hz, CH_2); 5.43 (6H, s, CH_2); 7.07 (3H, s, pz); 7.55 (3H, s, pz). IR (υ_{max} cm^{-1}): 3066(w), 2974(w), 1678(w), 1574(w), 1507(w), 1456(m), 1416(m), 1276(m), 1160(m), 1112(m), 989(s), 938(s), 843(s), 793(s), 762(m), 718(m), 645(m), 604(s), 569(m).

Elemental analysis for the tris(4-I-pz) [$C_{24}H_{27}N_6I$] was found (%) C = 36.47, H = 3.52, N = 10.45; Calculated (%) C = 36.95, H = 3.49, N = 10.77. X-ray quality single crystals were grown by slow evaporation from dichloromethane solution.

Synthesis and Characterizations of [ligand-PA] adducts

Synthesis of [1](PA) ($C_{48}H_{43}N_9O_7$)

31.5 mg (0.05 mmol) T(4-Ph)pz and 11.4 mg (0.05 mmol) were dissolved in 7 mL $CHCl_3$ or acetone and stirred 10 minutes at room temperature. Yield: 30 mg (70 %). ^{1}H-NMR (ppm, $CDCl_3$): 1.06 (9H, t, CH_3); 2.81 (6H, q, CH_2); 5.53 (6H, s, CH_2); 7.24-7.36 (18H phenyl+pz); 7.30 (1H, s, -OH_{PA}); 9.13 (2H, s, -CH_{PA}) phenyl); 7.85 (3H, s, pz). X-ray quality golden yellow colored single crystals were obtained by slow evaporation of the reaction solution.

Synthesis of [2] $(PA)_2$ ($C_{60}H_{47}Cl_3N_{15}O_{21}$)

7.8 mg (0.01 mmol) T-4-(4-NO_2-Ph)pz and 6.8 mg (0.03 mmol) were dissolved in 7 mL $CHCl_3$ and stirred 2 minutes at room temperature. Yield: 8 mg (68 %). ^{1}H-NMR (ppm, $CDCl_3$): 1.04 (9H, t, CH_3); 2.82 (6H, q, CH_2); 5.52 (6H, s, CH_2); 7.23 – 7.38 (15H, m, phenyl + pz); 7.84 (3H, s, pz); 7.36 (2H, s, -OH_{PA}); 9.13 (4H, s, -CH_{PA}). X-ray quality golden yellow colored single crystals were obtained by slow evaporation of the reaction solution.

Synthesis of [1] $(PA)_3$ ($C_{63}H_{51.5}N_{16.5}O_{24.5}$)

31.5 mg (0.05 mmol) T(4-Ph)pz and 33.4 mg (0.15 mmol) were dissolved in 7 mL $CHCl_3$ or acetone and stirred 10 minutes at room temperature. Yield: 50 mg (75 %). ^{1}H-NMR (ppm, $CDCl_3$): 1.07 (9H, t, CH_3); 2.81 (6H, q, CH_2); 5.57 (6H, s, CH_2); 7.23-7.36 (18H phenyl+pz); 7.38 (3H, s, -OH_{PA}); 9.14 (6H, s, -CH_{PA}) phenyl); 7.89 (3H, s, pz). X-ray quality golden yellow colored single crystals were obtained by slow evaporation of the reaction solution.

Figures:

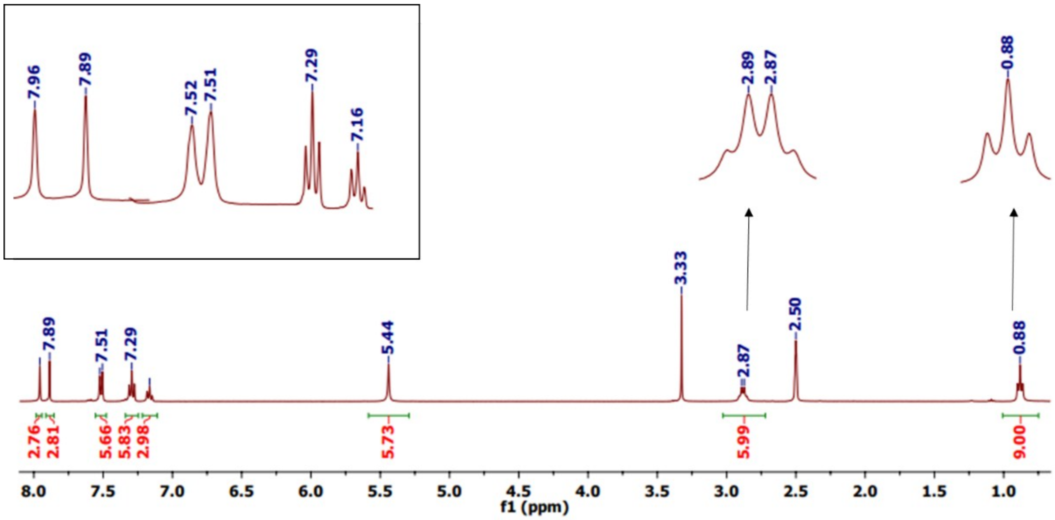

Fig. S1. *^{1}H NMR spectrum of compound **1**, DMSO-d$_6$. (Insert in blackbox : Expanded aromatic region)*

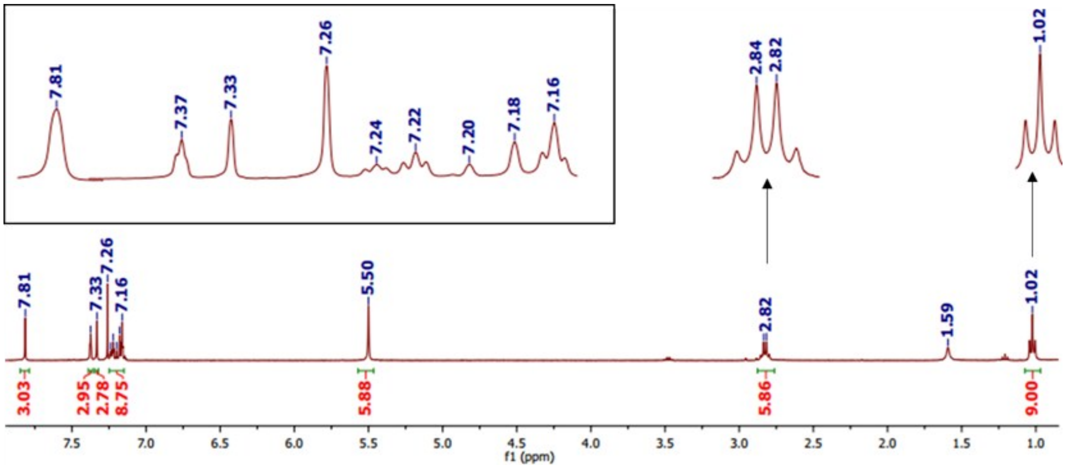

Fig. S2. *^{1}H NMR spectrum of compound **3**, CDCl$_3$ (Insert in blackbox : Expanded aromatic region)*

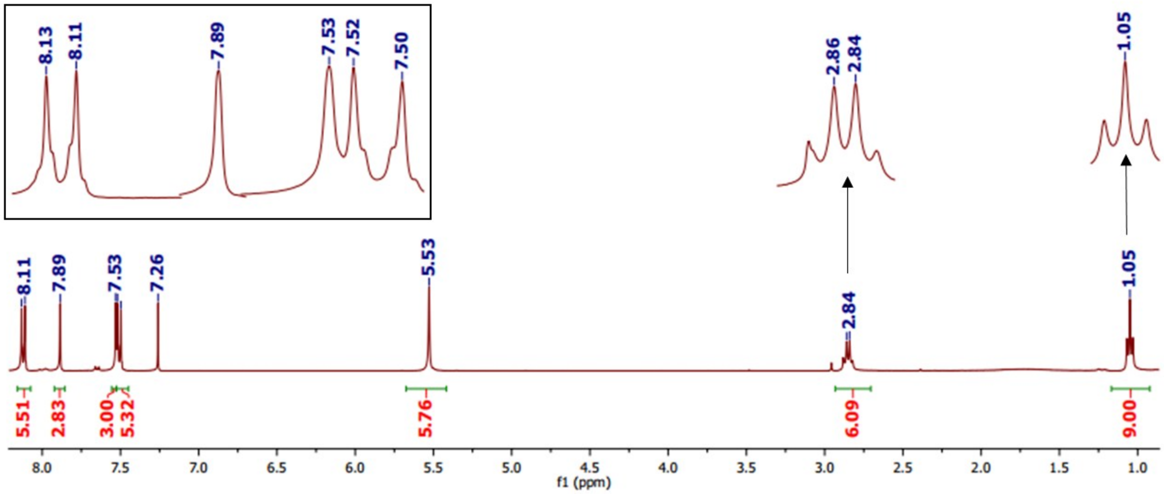

Fig. S3. *^{1}H NMR spectrum of compound* ***4****, $CDCl_3$ (Insert in blackbox: Expanded aromatic region).*

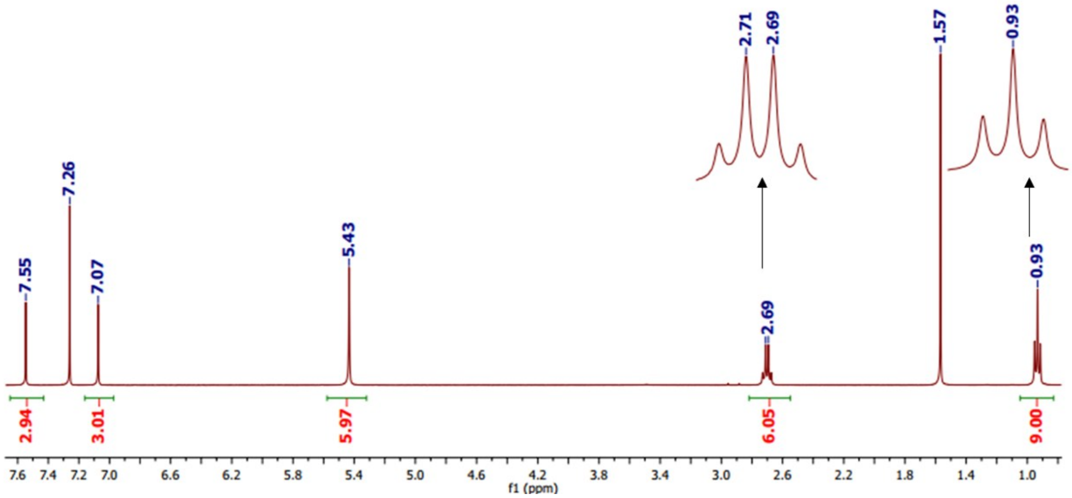

Fig. S4. *^{1}H NMR spectrum of compound* ***5****, $CDCl_3$*

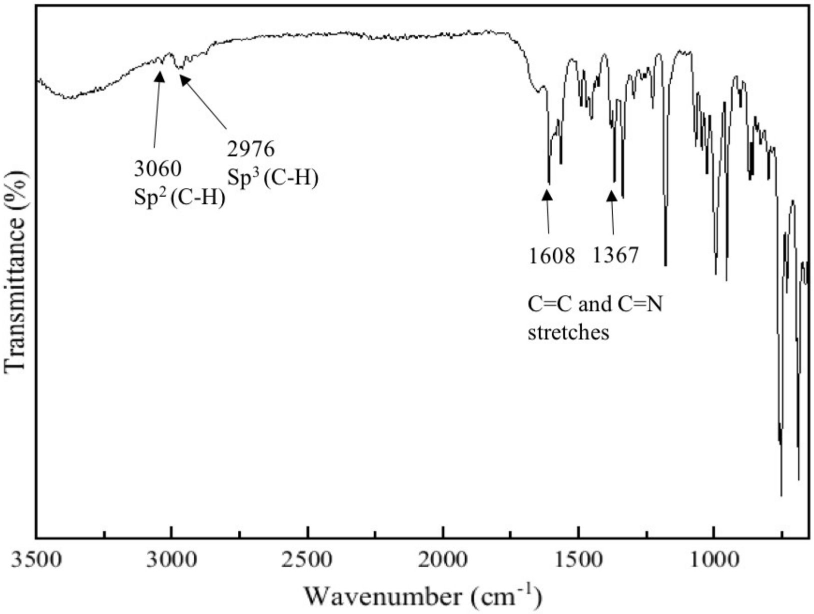

Fig. S5. *IR spectrum of compound **1**.*

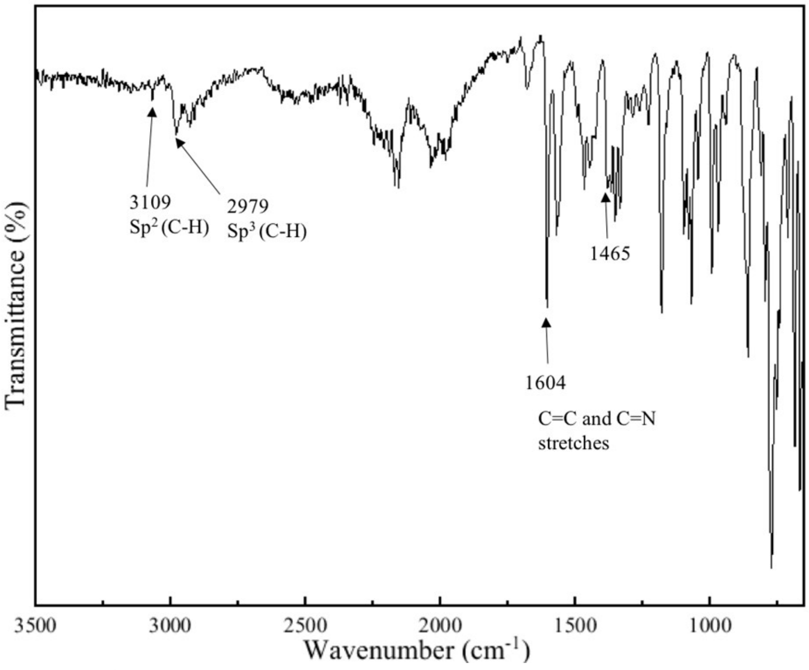

Fig. S6. *IR spectrum of compound **3**.*

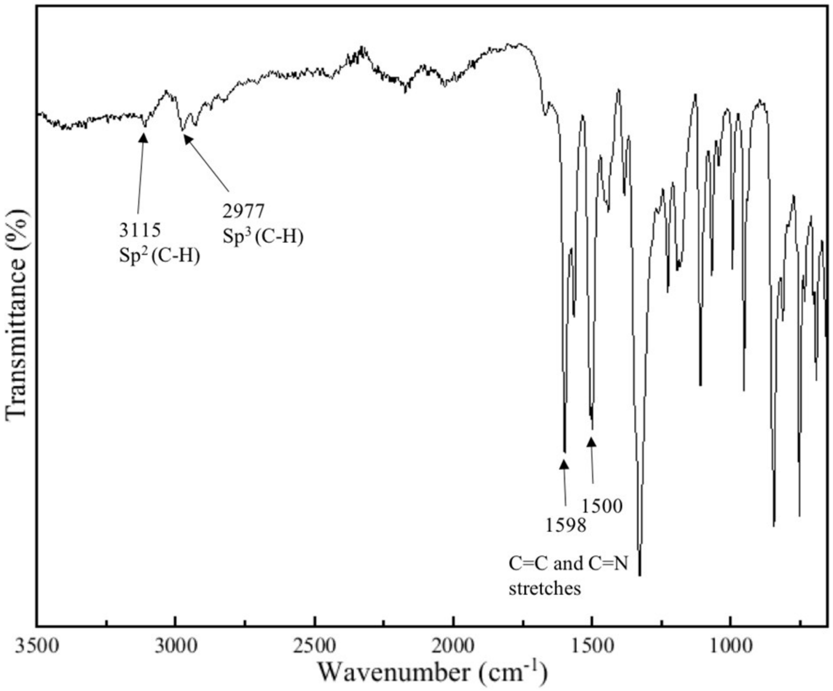

Fig. S7. *IR spectrum of compound **4**.*

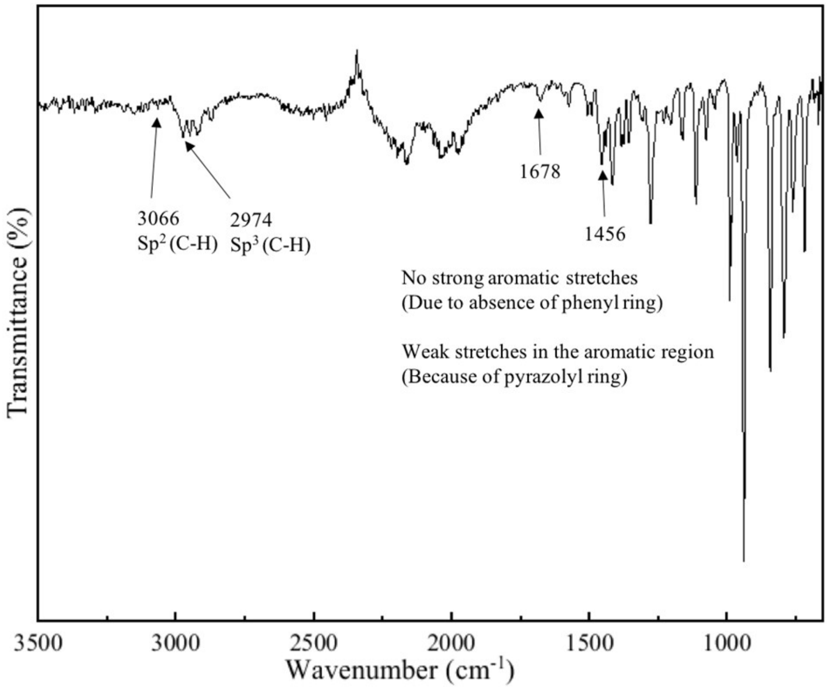

Fig. S8. *IR spectrum of compound **5**.*

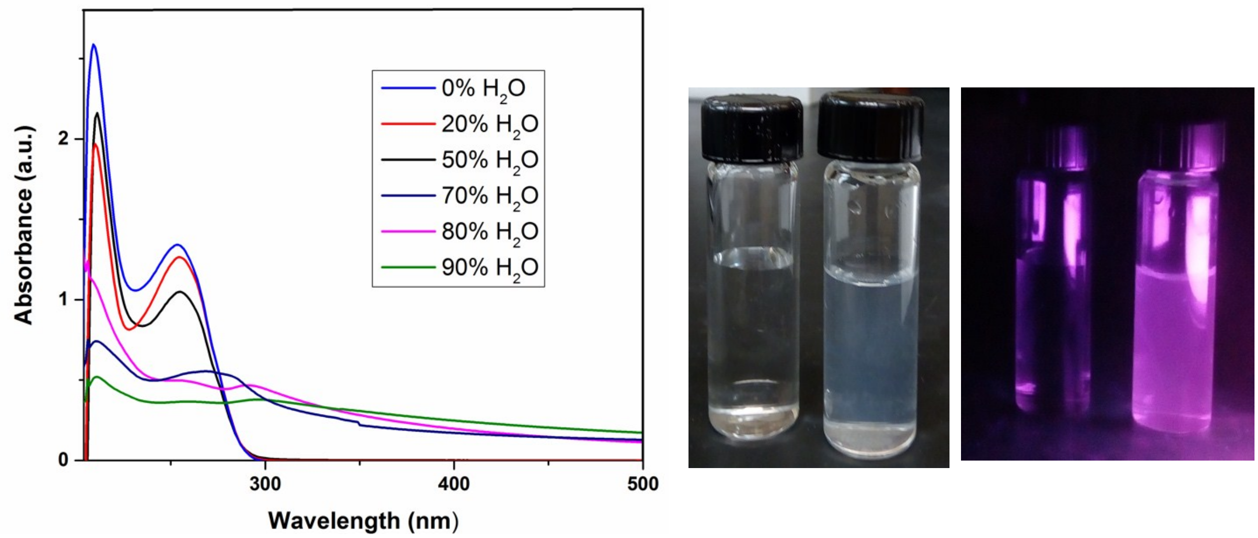

Fig. S9. *(a) UV – visible spectra of* ***2*** *in THF with the addition of water (0 to 90%). Photographs of* ***3*** *before (b) and after (c) in THF and THF/H_2O (20:80) mixture.*

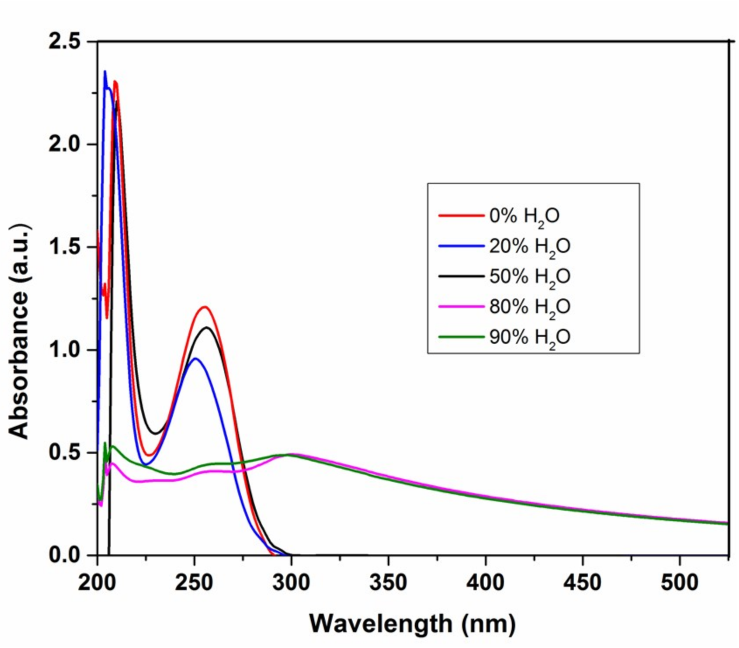

Fig. S10. *UV – visible spectra for* ***1*** *in THF with the gradual addition of water from 0 to 90%.*

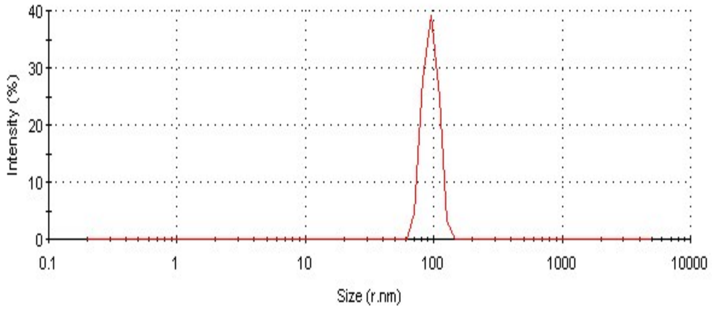

Fig. S11. *DLS data for the aggregates of* ***1*** *(15 µM) in THF/H_2O (20:80) mixture.*

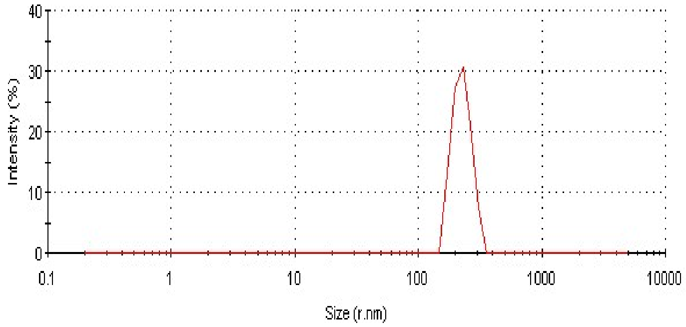

Fig. S12. *DLS data for the aggregates of* ***2*** *(15 µM) in THF/H_2O (20:80) mixture.*

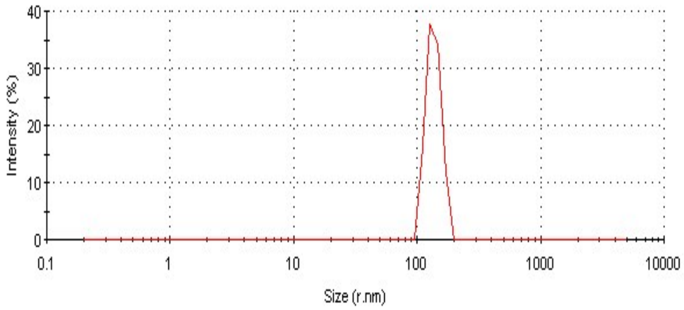

Fig. S13. *DLS data for the aggregates of* ***3*** *(15 µM) in THF/H_2O (20:80) mixture.*

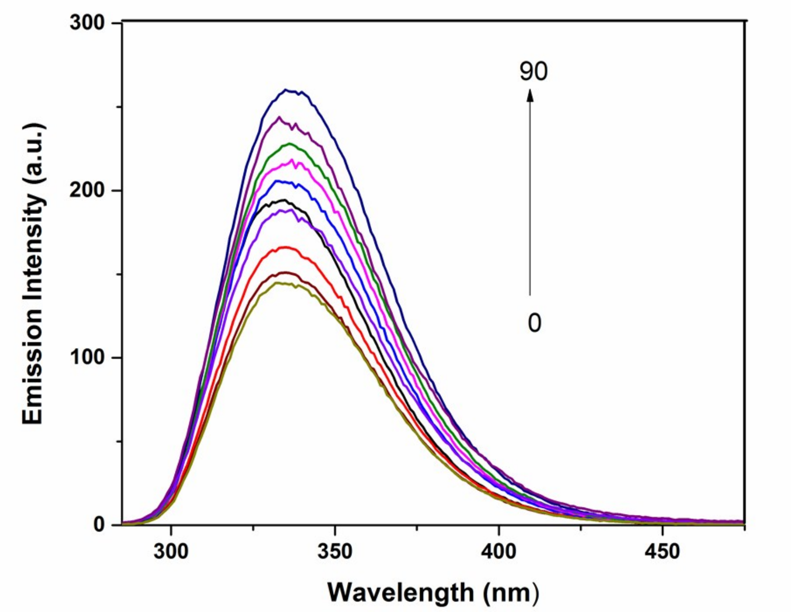

Fig. S14. *Fluorescence spectra of **2** (15 µM) with the addition of water from 0 to 90% into THF.*

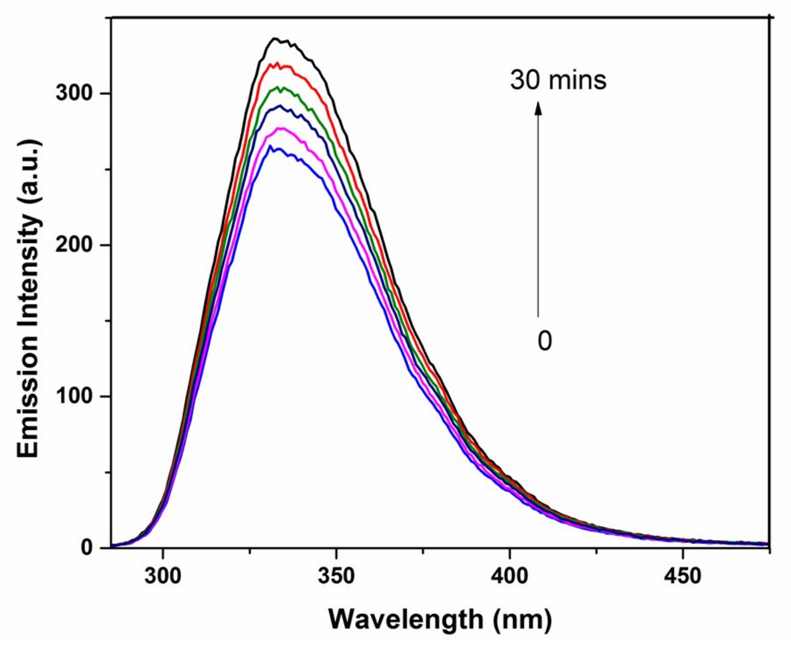

Fig. S15. *Fluorescence spectra of **2** (15 µM) in a THF/H_2O mixture (10:90 v/v) at different aging times; (Δt = 5 min).*

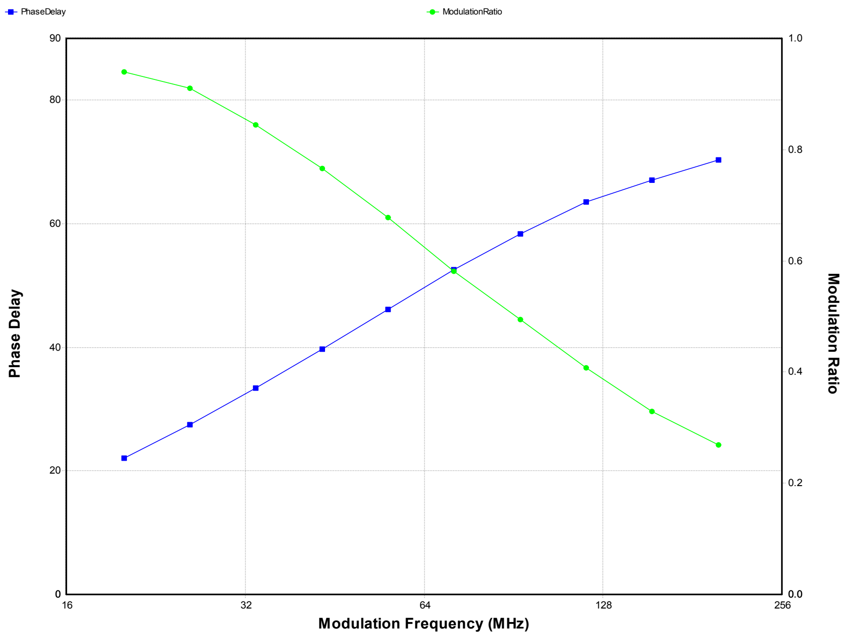

Fig.S16. *Frequency modulation data for **2** in THF; (τ = 1.2 ns).*

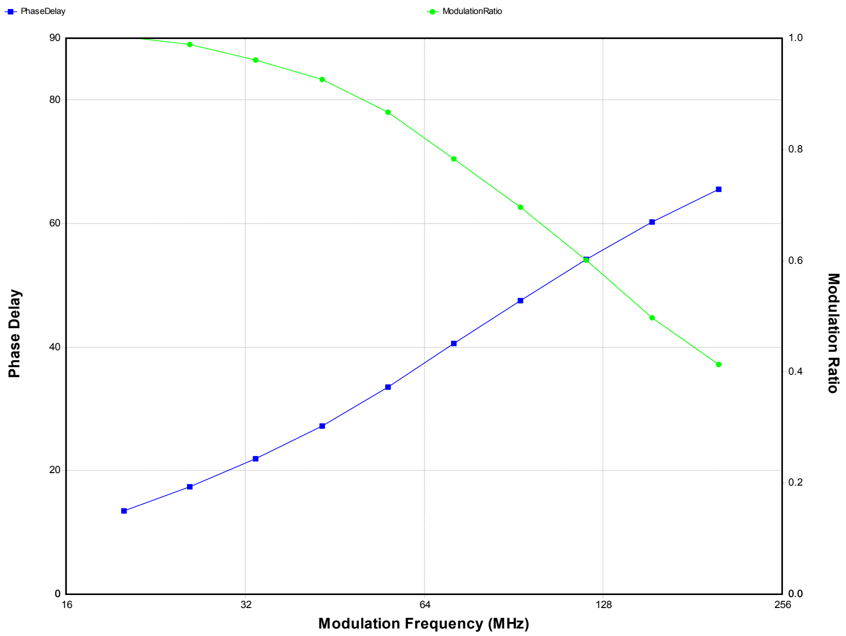

Fig.S17. *Frequency modulation data for 2 in THF/H_2O (10:90) mixture; (τ = 1.8 ns).*

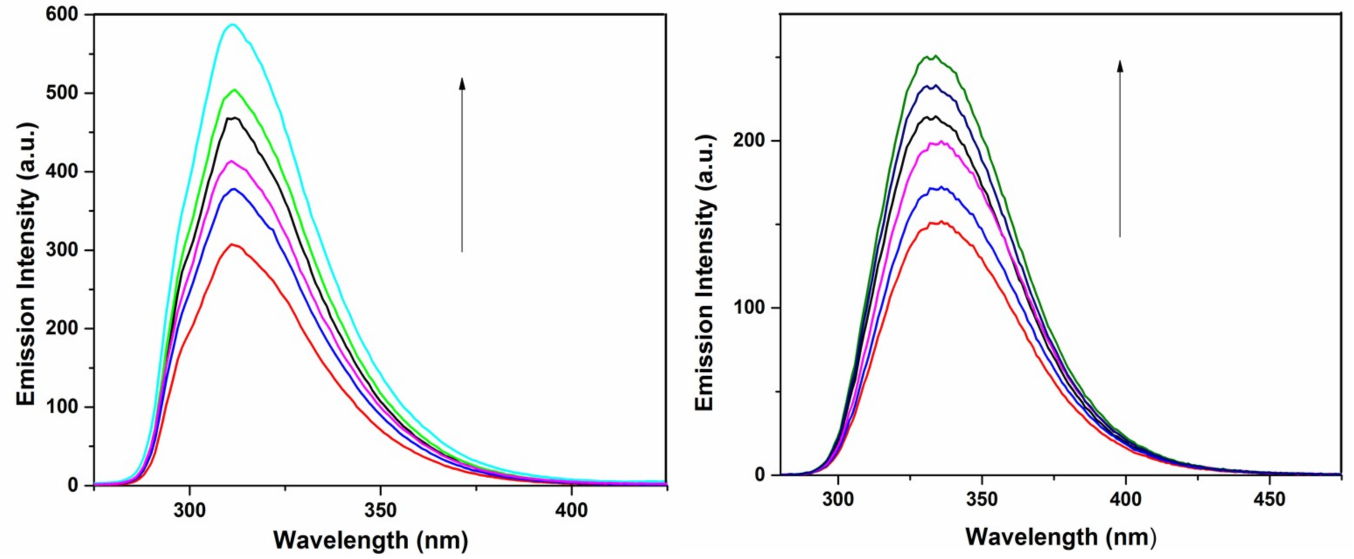

Fig. S18. *Variation of fluorescence intensity of compound* ***1*** *&* ***2*** *(15 μM) in THF/ethylene glycol (EG) mixture (0, 20, 40, 60, 80 & 90 volume fraction of EG in THF).*

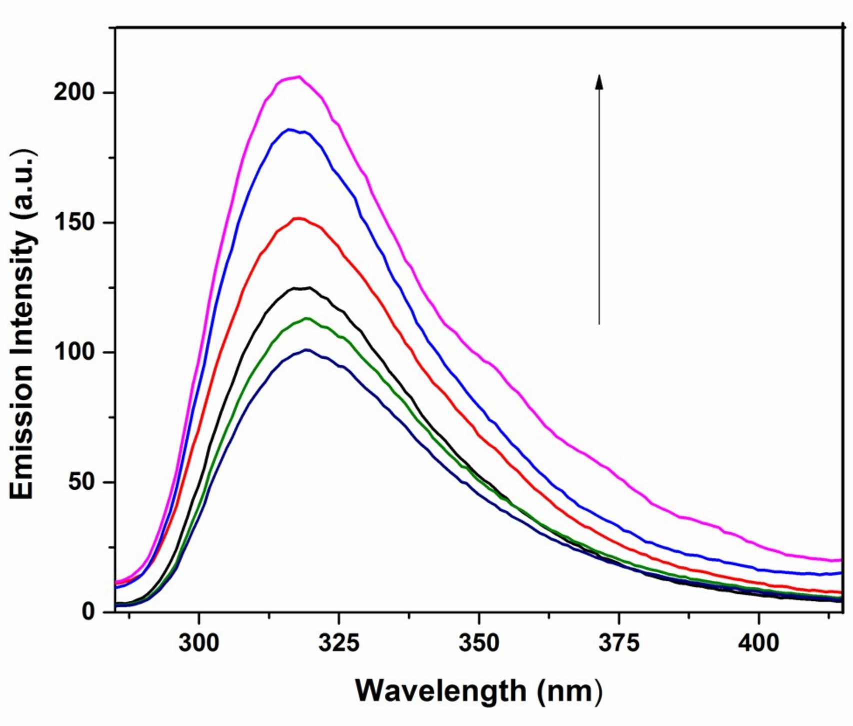

Fig. S19. *Variation of fluorescence intensity of compound **3** (15 µM) in THF/ethylene glycol (EG) mixture (0, 20, 40, 60, 80 & 90 volume fraction of EG in THF).*

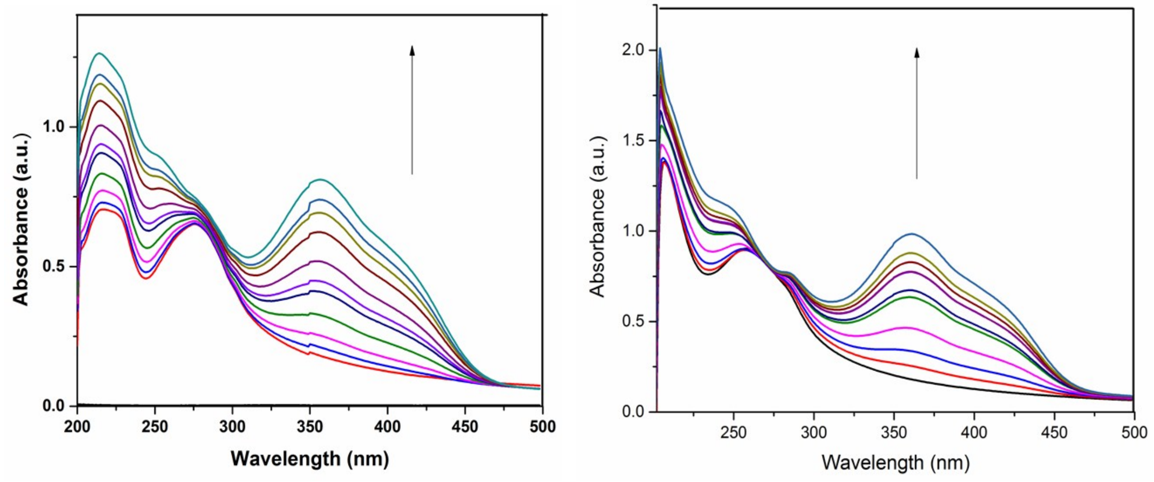

Fig. S20. *Absorption spectral changes of **1** & **2** (15 µM) in THF/H$_2$O (20:80) with the addition of PA (0 to 20 µM).*

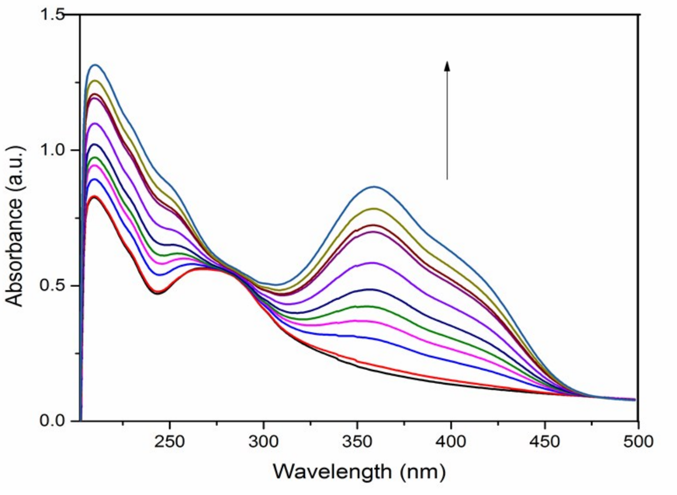

***Fig. S21**. Absorption spectral changes of **3** (15 µM) in THF/H$_2$O (20:80) with the addition of PA (0 to 20 µM).*

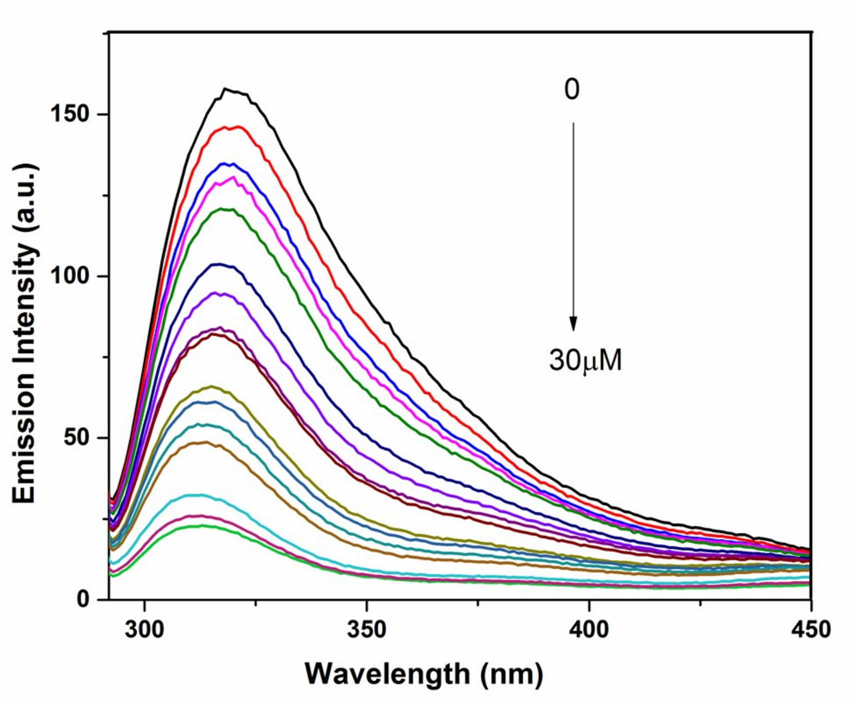

Fig. S22. *Emission spectra of* ***3*** *(15μM) in THF/H_2O (20:80) upon addition of PA from 0 to 30 μM.*

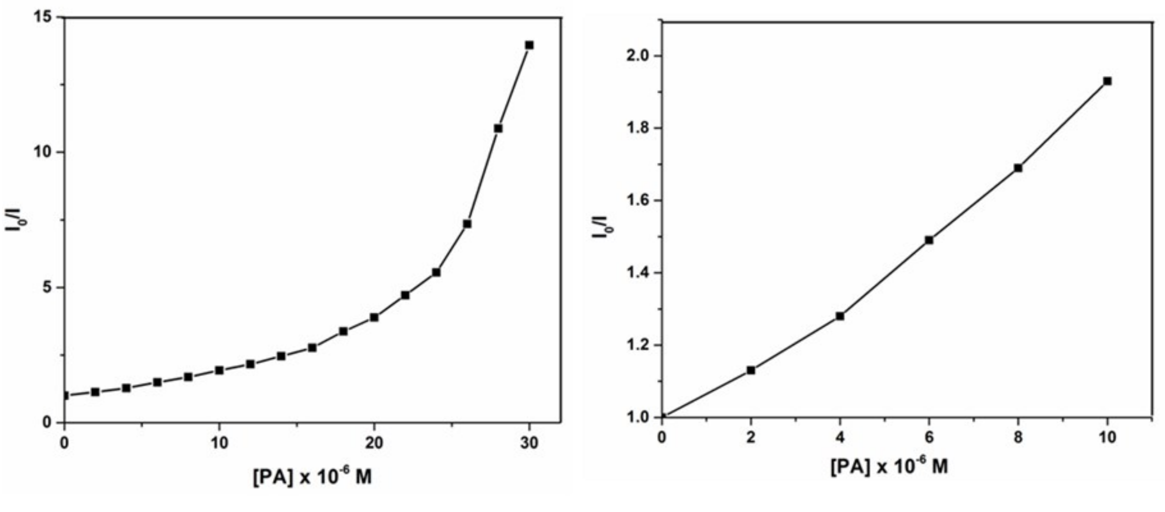

(a) **(b)**

Fig. S23. *(a) Stern-Volmer plot for the complex* ***1*** *with PA (b) SV plot obtain at lower concentration of PA.*

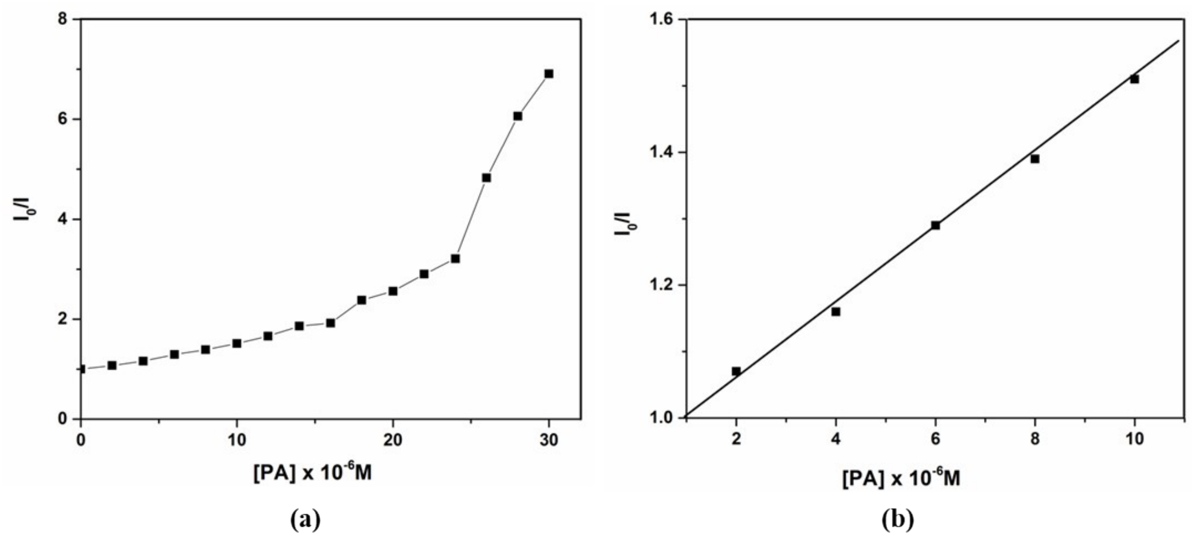

Fig. S24. *(a) Stern-Volmer plot for the complex **3** with PA (b) SV plot obtain at lower concentration of PA.*

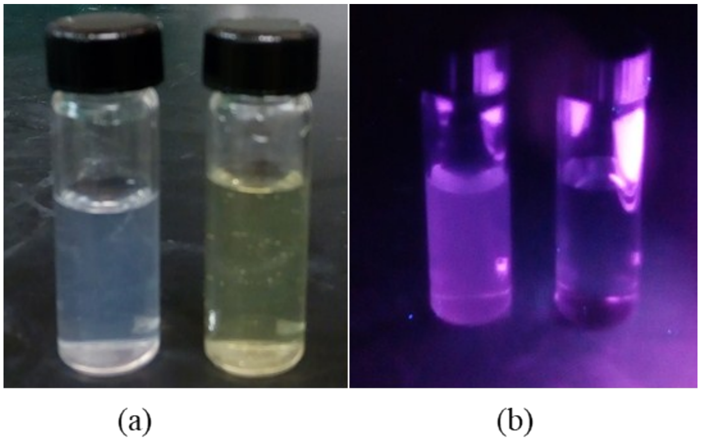

Fig. S25. *Photographs taken before (A) Complex **2** and **2**+PA after (B) Compound **2** and **2**+ PA.*

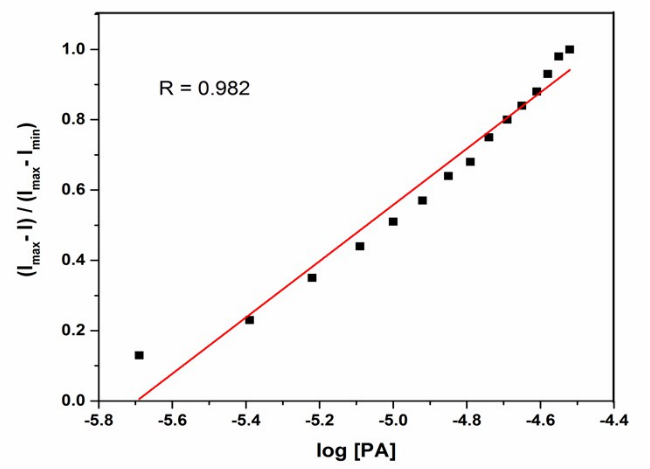
R = 0.982
$(I_{max} - I) / (I_{max} - I_{min})$
0.0
0.2
0.4
0.6
0.8
1.0
-5.8
-5.6
-5.4
-5.2
-5.0
-4.8
-4.6
-4.4
log [PA]

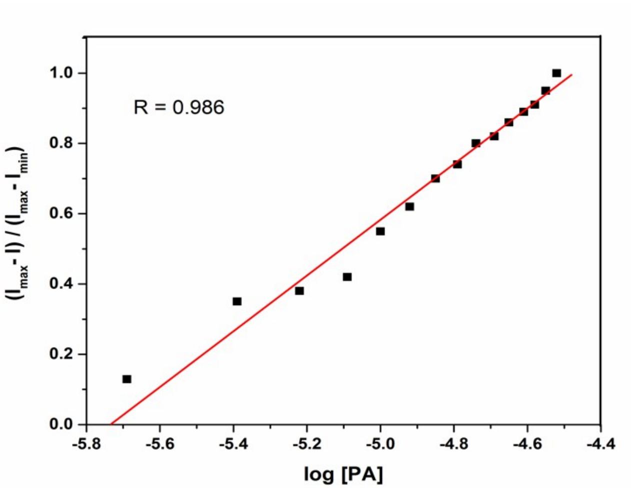
R = 0.986
$(I_{max} - I) / (I_{max} - I_{min})$
0.0
0.2
0.4
0.6
0.8
1.0
-5.8
-5.6
-5.4
-5.2
-5.0
-4.8
-4.6
-4.4
log [PA]

***Fig. S26.* (*I*$_{max}$-I)/(I$_{max}$-I$_{min}$) vs log [PA] for *1* (left) and *2* (right).**

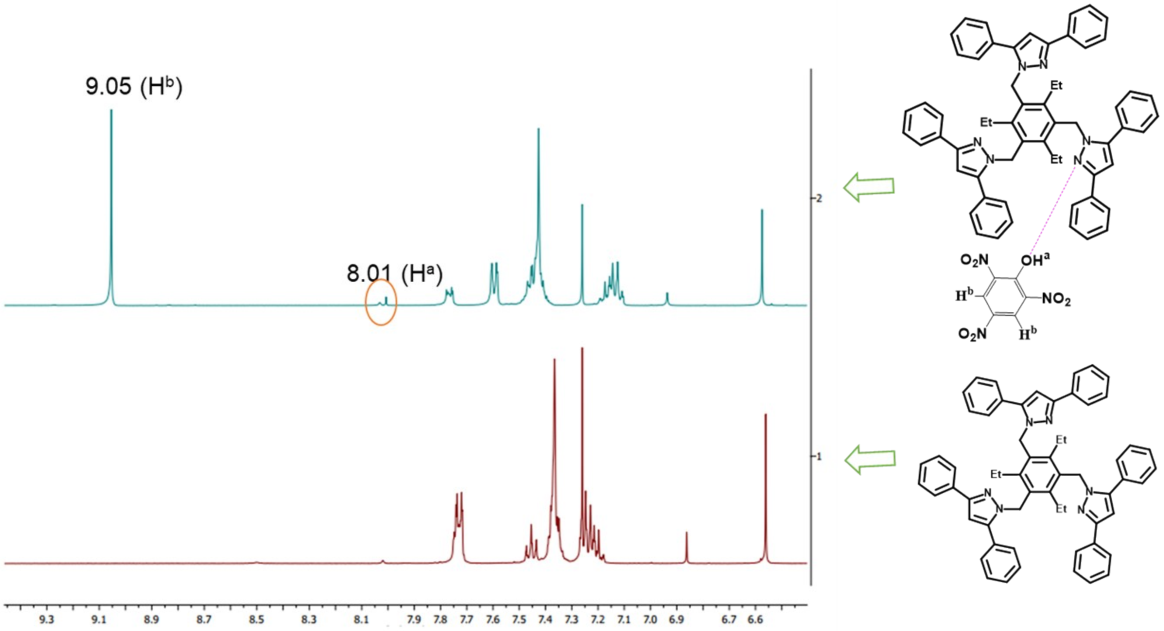

Fig. S27. *Partial* ^{1}*H-NMR spectra of* ***2*** *and* ***2****-PA.*

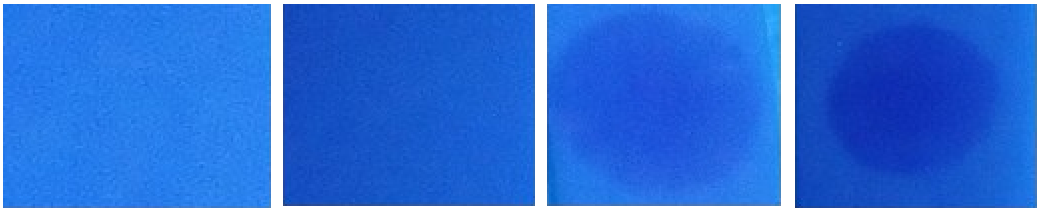

0 min **5 min** **10 min** **20min**

Fig. S28. *Photographs of compound* ***2*** *impregnated test paper strips upon exposure to the vapors of PA.*

Tables

Table S1. Crystallographic data of *compounds* ***(1), (3) – (5)***

Identification code	T(4ph)pz (**1**)	T4(3Clph)pz (**3**)	T4(4NO$_2$ph)pz (**4**)	T(4I)pz (**5**)
Empirical formula	$C_{42}H_{42}N_6$	$C_{42}H_{39}Cl_3N_6$	$C_{42}H_{39}N_9O_6$	$C_{24}H_{27}I_3N_6$
Formula weight	630.84	734.14	765.82	780.21
Temperature/K	300.73	293(2)	298	298
Crystal system	Monoclinic	monoclinic	monoclinic	orthorhombic
Space group	$P2_1/n$	$P2_1/n$	$P2_1/c$	$P2_12_12_1$
a/Å	9.9811(5)	10.1425(5)	11.5556(9)	9.3404(4)
b/Å	15.2986(7)	16.1254(8)	28.763(2)	14.3252(6)
c/Å	23.0545(11)	23.3070(12)	12.7786(10)	22.6650(10)
α/°	90	90	90	90
β/°	101.511(2)	101.9640(10)	116.596(2)	90
γ/°	90	90	90	90
Volume/Å^3	3449.5(3)	3729.1(3)	3797.9(5)	3032.6(2)
Z	4	4	4	4
ρ_{calc}g/cm^3	1.2146	1.308	1.339	1.709
μ/mm^{-1}	0.073	0.285	0.093	3.113
F(000)	1344.5	1536	1608.0	1488.0
Crystal size/mm^3	0.23 × 0.218 × 0.197	0.254 × 0.217 × 0.143	0.386 × 0.1 × 0.071	0.207 × 0.073 × 0.07
Radiation	Mo Kα (λ = 0.71073)	MoKα (λ = 0.71073)	Mo Kα (λ = 0.71073)	MoKα (λ = 0.71073)
2Θ range for data collection/°	5.54 to 52.86	5.926 to 52.866	5.796 to 50.246	5.966 to 50.246
Index ranges	$-12 \le h \le 11$, $-18 \le k \le 19$, $-28 \le l \le 28$	$-12 \le h \le 12$, $-20 \le k \le 20$, $-29 \le l \le 28$	$-13 \le h \le 13$, $-34 \le k \le 34$, $-15 \le l \le 15$	$-11 \le h \le 11$, $-17 \le k \le 16$, $-27 \le l \le 27$

Reflections collected	59428	65441	64897	52505
Independent reflections	7013 [R_{int} = 0.0742, R_{sigma} = 0.0583]	7635 [R_{int} = 0.0682, R_{sigma} = 0.0549]	6770 [R_{int} = 0.1674, R_{sigma} = 0.1295]	5389 [R_{int} = 0.0907, R_{sigma} = 0.0661]
Data/restraints/parameters	7013/0/436	7635/0/463	6770/0/517	5389/0/311
Goodness-of-fit on F^2	1.072	1.015	1.008	1.040
Final R indexes [I>=2σ (I)]	R_1 = 0.0688, wR_2 = 0.1213	R_1 = 0.0700, wR_2 = 0.1591	R_1 = 0.0932, wR_2 = 0.1683	R_1 = 0.0458, wR_2 = 0.0747
Final R indexes [all data]	R_1 = 0.1385, wR_2 = 0.1454	R_1 = 0.1365, wR_2 = 0.1893	R_1 = 0.2302, wR_2 = 0.2173	R_1 = 0.0923, wR_2 = 0.0842
Largest diff. peak/hole / e Å^{-3}	0.40/-0.43	0.35/-0.47	0.19/-0.20	0.54/-0.38

Table S2. ^{1}H-NMR shifts (ppm) of 1, 3 - 5.

Compounds	A	B	C	Ph ring	Pz
(solvent)	(9H, *t*)	(6H, *q*)	(6H, *s*)	protons	protons
1 (DMSO-d_6)	0.88	2.88	5.44	7.16 (3H, *t*), 7.29 (6H, *t*), 7.51 (6H, *d*)	7.89 (3H, *s*),
3 ($CDCl_3$)	1.02	2.83	5.50	7.15 – 7.25 (9H, *m*), 7.37 (3H, *s*)	7.33 (3H, *s*), 7.81 (3H, *s*)
4 ($CDCl_3$)	1.05	2.85	5.53	7.51 (6H, *d*), 8.12 (6H, *d*)	7.53 (3H, *s*), 7.89 (3H, *s*)
5 ($CDCl_3$)	0.93	2.71	5.43		7.07 (3H, *s*), 7.55 (3H, *s*)

A = ethyl (-CH_3), B = ethyl (-CH_2), C = (-CH_2, between benzene moiety and pyrazole)

Table S3. ^{1}*H NMR spectra (in ppm) of ligands (1, 2, 3) and ligands + picric acid in* $CDCl_3$.

Compds	A (9H,t)	B (6H,q)	C(6H,s)	D[3H,s,Pz-C(3)]	[18H, benzene ring + Pz-C(5)]	PA (s, -CH)	PA(s, OH)
PA						9.20	11.97
[**1**]	1.05	2.82	5.50	7.82	7.25 (9H), 7.34 + 7.36 (9H)		
[**1**] (PA)	1.06	2.81	5.53	7.85	7.24 (9H), 7.30 (3H), 7.34 + 7.36 (6H)	9.13	7.30
[**1**] $(PA)_2$	1.06	2.81	5.54	7.86	7.24 (9H), 7.34 (9H)	9.15	7.32
[**1**] $(PA)_3$	1.07	2.81	5.57	7.89	7.23 (6H), 7.27 (3H), 7.36 (9H)	9.14	7.38

Compds	A (9H,t)	B (6H,q)	C (6H,s)	D [3H,s,Pz-C(4)]	Benzene ring (30H)	PA (s, -CH)	PA(s,-OH)
[**2**]	0.65	2.56	5.25	6.56	7.18 - 7.24 (6H), 7.36 (15H), 7.43 - 7.47 (3H), 7.73(6H)		
[**2**] (PA)	0.73	2.59	5.29	6.57	7.11 - 7.17 (9H), 7.43 (12H), 7.59(6H), 7.77 (3H)	9.05	8.01

Compds	A (9H,t)	B (6H,q)	C (6H,s)	D [3H,s,Pz-C(3)]	[15H, benzene ring + Pz-C(5)]	PA (s, CH)	PA(s,-OH)
[**3**]	1.02	2.82	5.50	7.81	7.16 - 7.24 (9H), 7.37 (3H), 7.33 (3H)		
[**3**] (PA)	1.04	2.82	5.52	7.84	7.15-7.23 (9H), 7.36 - 7.38 (6H)	9.16	7.36

Table S4. Crystallographic data of compounds [1] (PA), [3] (PA)$_2$ and [1] (PA)$_{3.5}$.

Identification code	[**1**](PA)	[**3**](PA)$_2$	[**1**](PA)$_{3.5}$
Empirical formula	$C_{48}H_{43}N_9O_7$	$C_{60}H_{47}Cl_3N_{15}O_{21}$	$C_{63}H_{51.5}N_{16.5}O_{24.5}$
Formula weight	857.91	1420.47	1431.70
Temperature/K	298(2)	296.69	298
Crystal system	Monoclinic	monoclinic	monoclinic
Space group	*C2/c*	*P2$_1$/m*	*P2/c*
a/Å	8.0177(17)	13.3120(6)	20.8248(9)
b/Å	25.274(5)	20.1594(9)	14.9586(7)
c/Å	46.068(10)	14.3878(6)	22.5799(11)
α/°	90	90	90
β/°	94.034(3)	110.6820(10)	113.6630(10)
γ/°	90	90	90
Volume/Å^3	9312(3)	3612.3(3)	6442.5(5)
Z	8	2	4
ρ_{calc}g/cm^3	1.224	1.306	1.476
μ/mm^{-1}	0.084	0.207	0.116
F(000)	3600.0	1462.0	2964.0
Crystal size/mm^3	0.159 × 0.12 × 0.101	0.201 × 0.11 × 0.101	0.2 × 0.18 × 0.16
Radiation	MoKα (λ = 0.71073)	MoKα (λ = 0.71073)	MoKα (λ = 0.71073)
2Θ range for data collection/°	5.806 to 50.436	5.776 to 50.122	5.792 to 49.634
Index ranges	$-9 \leq h \leq 9$, $-30 \leq k \leq 30$, $-51 \leq l \leq 53$	$-15 \leq h \leq 15$, $-23 \leq k \leq 24$, $-17 \leq l \leq 17$	$-24 \leq h \leq 24$, $-17 \leq k \leq 17$, $-26 \leq l \leq 26$
Reflections collected	55487	61389	133126

Independent reflections	8261 [R_{int} = 0.2023, R_{sigma} = 0.1750]	6589 [R_{int} = 0.0381, R_{sigma} = 0.0250]	11065 [R_{int} = 0.1508, R_{sigma} = 0.0944]
Data/restraints/parameters	8261/0/589	6589/0/499	11065/0/940
Goodness-of-fit on F^2	1.023	1.136	1.014
Final R indexes [I>=2σ (I)]	R_1 = 0.1315, wR_2 = 0.2509	R_1 = 0.0813, wR_2 = 0.2292	R_1 = 0.1015, wR_2 = 0.2223
Final R indexes [all data]	R_1 = 0.2645, wR_2 = 0.3036	R_1 = 0.1110, wR_2 = 0.2516	R_1 = 0.2116, wR_2 = 0.2780
Largest diff. peak/hole / e $Å^{-3}$	0.35/-0.34	1.03/-0.47	1.24/-0.58

References:

1. (a) N. Koch and M. Mazik, *Synthesis* 2013**, 45**, 3341-3348; (b) T. M. Jonah, L. Mathivathanan, A. N. Morozov, A. M. Mebel, R. G. Raptis and K. Kavallieratos, *New J. Chem.* 2017, **41**, 14835-14838; (c) A. Vacca, C. Nativi, M. Cacciarini, R. Pergoli and S. Roelens, *J. Am. Chem. Soc.* 2004, **126**, 16456-16465.
2. J. Olguín and S. Brooker, *New J. Chem.* 2011**, 35**, 1242-1253.

3. B. Roy, A. K. Bar, B. Gole, and P. S. Mukherjee, *J. Org. Chem.* 2013, **78**, 1306−1310.
4. G. M. Sheldrick, *Acta Crystallogr. Sect. A* 2015**, 71**, 3-8.
5. O. V. Dolomanov, L. J. Bourhis, R. J. Gildea, J. A. Howard and H. Puschmann, *J. Appl. Cryst.* 2009**, 42**, 339-341.
6. G. M. Sheldrick, *Acta Crystallogr. Sect. C* 2015**, 71**, 3-8.
7. A. L. Spek, *Acta Crystallogr. Sect. C* 2015, **71**, 9-18.
8. J.-D. Chai and M. Head-Gordon, *Phys. Chem. Chem. Phys.* 2008, **10**, 6615-6620.
9. (a) M. E. Casida, C. Jamorski, K. C. Casida and D. R. Salahub, *J. Chem. Phys.* 1998, **108**, 4439-4449; (b) R. E. Stratmann, G. E. Scuseria and M. J. Frisch, *J. Chem. Phys.* 1998, **109**, 8218-8224.
10. Gaussian09, R. A., 1, MJ Frisch, GW Trucks, HB Schlegel, GE Scuseria, MA Robb, JR Cheeseman, G. Scalmani, V. Barone, B. Mennucci, GA Petersson et al., Gaussian. *Inc., Wallingford CT* 2009**, 121**, 150-166.